ELECTRICAL PROPERTIES OF VACUUM EVAPORATED SILICON OXIDE FILMS

By L. Żdanowicz and K. Zielińska

Institute of Solid State Physics, Polish Academy of Sciences, Zabrze*

(Received November 12, 1976)

The measurements of electrical conductivity, I—V characteristics and the dielectric constant have been performed for Me—SiO_x—Me structures obtained by thermal vacuum evaporation. Films were evaporated in the "sandwich" configuration using Al, Ag, Au or Cu as electrodes. The I—V characteristics have been measured for external voltages 0—130 V and in the temperature range 90—300 K. The conductivity measurements have been performed both in dc and ac systems, for temperature from 80 to 520 K and for the frequency range $400-10^4$ Hz. Two regions can be noticed on the current-voltage characteristics owing to different conductivity mechanisms. The height of the potential barriers of the metal-dielectric boundary for different values of electric field F and for several temperatures were calculated from the plots $\log I = f(U^{1/2})$ with the assumption of Schottky emission. The activation energy of trapping levels was estimated from $\log \sigma - f(1/T)$ dependence as 0.16—0.19 eV. Also the normalization curve $J = (F^{1/2}T^{-1})$ was derived on the basis of $\log I$ versus $\log U$ characteristics, which indicates the presence of the Poole–Frenkel conduction mechanism. At low voltages and higher temperatures the Schottky mechanism is prefered.

1. Introduction

Electrical properties of dielectric thin films have been investigated by several authors (see [1–4] for example). However, there is a great discrepancy both between experimental results and their interpretation. This is due to the problems in preparing well-defined structures by commonly used methods i.e. evaporating and anodizing.

The majority of experimental works deal with electrical propertied measures in dc and ac systems as well. One of the most frequently investigated materials is silicon oxide. Different conduction mechanisms have been suggested for it in dc [1–4] and ac [5–7] systems. Some of these mechanisms are applicable for this films of other materials, too.

In silicon oxide films, the low-field and relatively high-temperature dc conductivity is mainly of ionic origin. It is characterized by relatively high activation energies and long-term polarization effects associated with the electrodes [7, 8].

* Address: Zakład Fizyki Ciała Stałego, PAN, Kawalca 3, 41-800 Zabrze, Poland.

For the case of high fields, the conductivity in silicon oxide is of the electronic type [9]. Many of the conductivity mechanisms are sensitive to the structure of films, thus deposition conditions and annealing are of great importance [5]. Even nine orders of magnitude differences can be observed [2]. ac properties, although to a lesser extent, are also structure dependent [7].

It is thus difficult to find the relation between theoretical and experimental results for the conductivity of silicon oxide films. For a typical experimental system the total conductivity depends on the number of independent mechanisms [10]. The achievement of stability and reproducibility is an important condition, the fulfillment of which is possible by very careful preparation and storing of films in a controlled environment.

2. *Experiment*

Thin film structures metal-SiO_x film-metal in sandwich configuration (Fig. 1) have been prepared on aircleaved mica and BK-7 glass substrates. The substrate temperatures were 293 K and 423 K. Evaporation was performed in a vacuum 10^{-5}torr. A tungsten

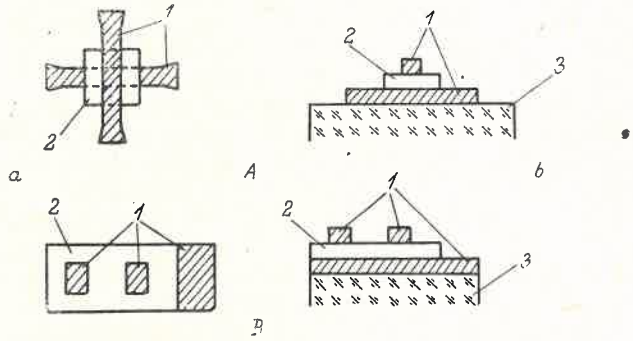

Fig. 1. Two types of evaporated sandwich systems: A — active surface ~1 mm², B — active surface ~12 mm², a — external view, b — cross-section, *1* — electrodes, *2* — SiO_x films, *3* — substrate

crucible was used. The thicknesses of SiO_x films measured by interference method, did not exceed 1.0 μm. The rate of deposition calculated from the known film thicknesses and time of evaporation was in the range 14—28 Å/s. Active surface areas of investigated structures varied from 1 mm² to 12 mm².

Two kinds of silicon monoxide have been used to prepare SiO_x films; that of Schuchardt (SiO 99%) and that of Balzers (SiO 99.8%). The starting material has been observed to have strong influence on the homogeneity of evaporated films. For SiO 99.8%, films of much higher homogeneity with a lower number of holes have been prepared. For the first kind of starting material (SiO 99%) in about 90% of structures the shorting was exhibited immediately after evaporation and for the second kind (SiO 99.8%) less than 10% od structures broke down.

Due to the constant number of broken-down structures it was possible to conclude that the distribution of defects is constant on the whole evaporated surface. Then it was

reasonable to assume that there is one defect responsible for shorting per about 10 mm² of surface area. For the derivation of more than 90% of the measurable structures an area of 1 mm² was chosen.

The second factor influencing the shorting of structures was the purity of the lower evaporated electrode. The application of the mask-exchanger allowed us to increase the active surface up to 12 mm².

As electrode materials we used aluminium, gold, silver and copper. The investigation of metal-SiO_x film-metal structures in the configuration of different electrodes allowed us to conclude that the most convenient material for electrodes is aluminium, which is characterized by a low temperature of evaporation, low surface mobility of atoms and is fine-grained as well [9, 11].

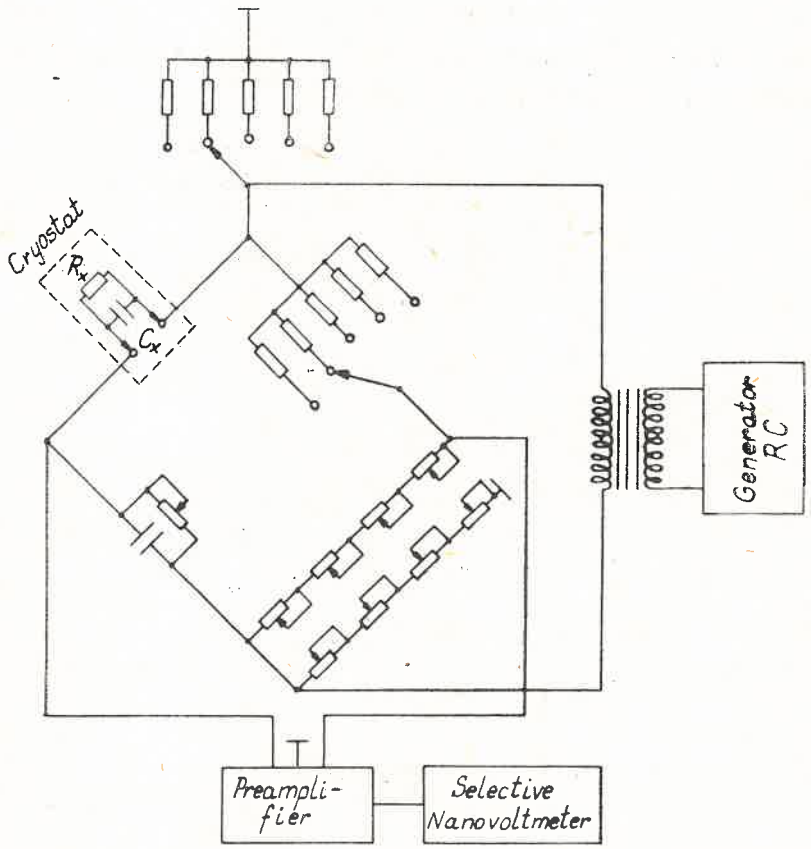

Fig 2. A block-scheme of the systems utilized in measurements of capacity and ac conductivity as a function of frequency

For the structure obtained, the dc current-voltage characteristics were derived for voltage in the range 0—130 V. The current intensity was measured over the range $1 \times 10^{-13} - 3 \times 10^{-5}$ A with the help of the electrometer (type 219, Unitra).

For temperature measurement the sample was held on the copper block and then placed in a dewar filled with liquid nitrogen. The temperature was measured with the help of a copper-constantan thermocouple.

The modified Wagner bridge [12] was used to investigate the slow-relaxation effects. The bridge was fed by the outer RC generator with continuously retuned frequency and regulated amplitude. The selective nanovoltmeter having an amplifier with symmetric input served as an index of equilibrium. Such a system allowed us to measure capacity and ac conducivity for the frequency range 10—10^4 Hz and for voltages on investigated structure no greater than 200 mV. The block-scheme of the system is presented in Fig. 2.

3. Results

3.1. Current-voltage characteristics

The current-voltage characteristics were determined for samples with different electrodes and over the temperature range 90—300 K.

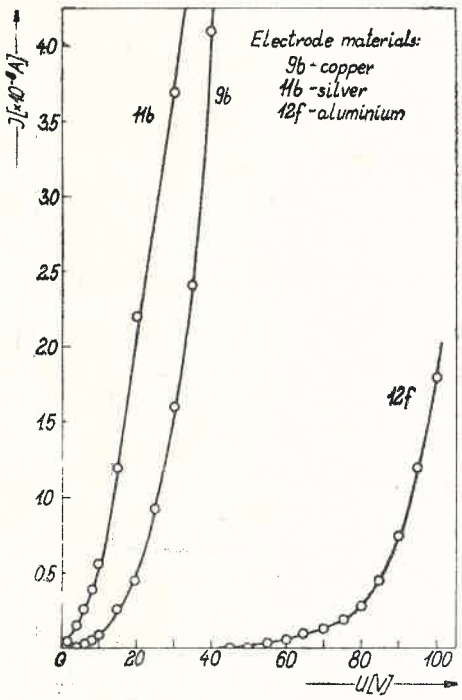

Fig. 3. Current-voltage characteristics for the samples with different electrodes

At low temperatures the current in investigated structures became established in about 1800 s when stationary voltage was applied. This was the reason for which during the investigation of I—V characteristics the current was measured after at least 30 s. The characteristics derived in such a manner suggest an unstable state for the dielectric.

The conductivity of a dielectric in an unstable state is usually explained in terms of Richardson-Schottky and Poole-Frenkel mechanisms [13].

In Fig. 3, three current-voltage characteristics are presented for samples with different electrodes. The samples with silver, gold and copper electrodes broke — down at a relatively low voltage: 11b — at $U = 25$ V, 9b — at $U = 40$ V, which corresponds to the field intensity $F = 37 \times 10^6$ V/m and $F = 8 \times 10^7$ V/m respectively. For the case of samples with aluminium electrodes no shorting was observed over the whole range of voltage applied (0—130 V).

In Fig. 4 the temperature dependence of I—V characteristics is presented. This dependence is very strong and increases with decreasing applied voltage. Servini and Jonscher [9]

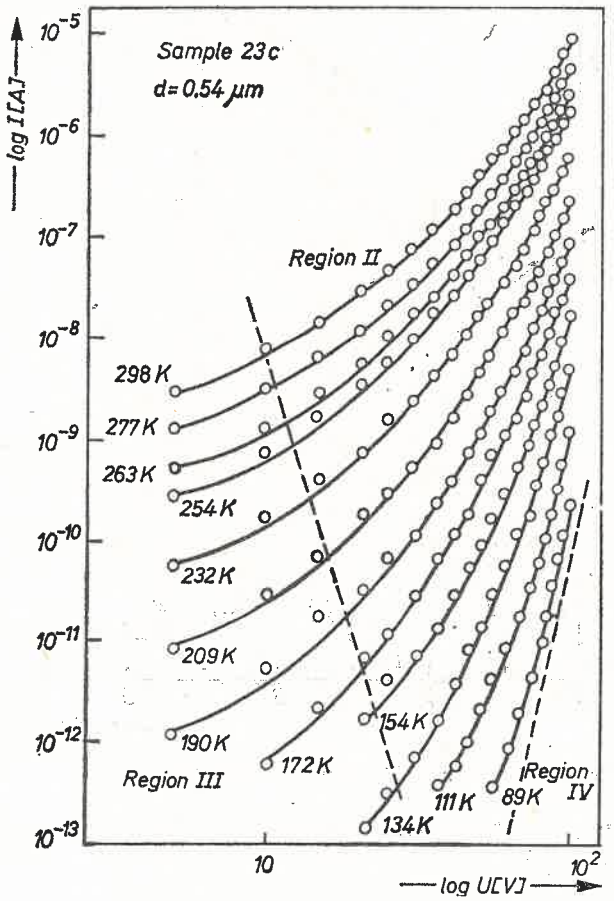

Fig. 4. Current-voltage characteristics for different temperatures in logarithmic scale

have presented the same type of characteristics on which they have distinguished four regions with different conductivity mechanisms. For our characteristics (Fig. 4) we can mark out their region II characterized by the linear dependence of $\log I$ on the square root of applied voltage and a part of region III which is described by the power law with

the index tending to 1.5. This distinction is due to the range of temperatures and voltage applied. Region II is an especially interesting one. I—V characteristics referring to this region are presented in Fig. 5. A linear sector is observed, the presence of which is usually explained in terms of the Richardson–Schottky or Poole–Frenkel emission.

Both types of emission are regulated by the external electric field. In the Richardson–Schottky emission the electrons are emitted from the metallic electrode and in Poole–

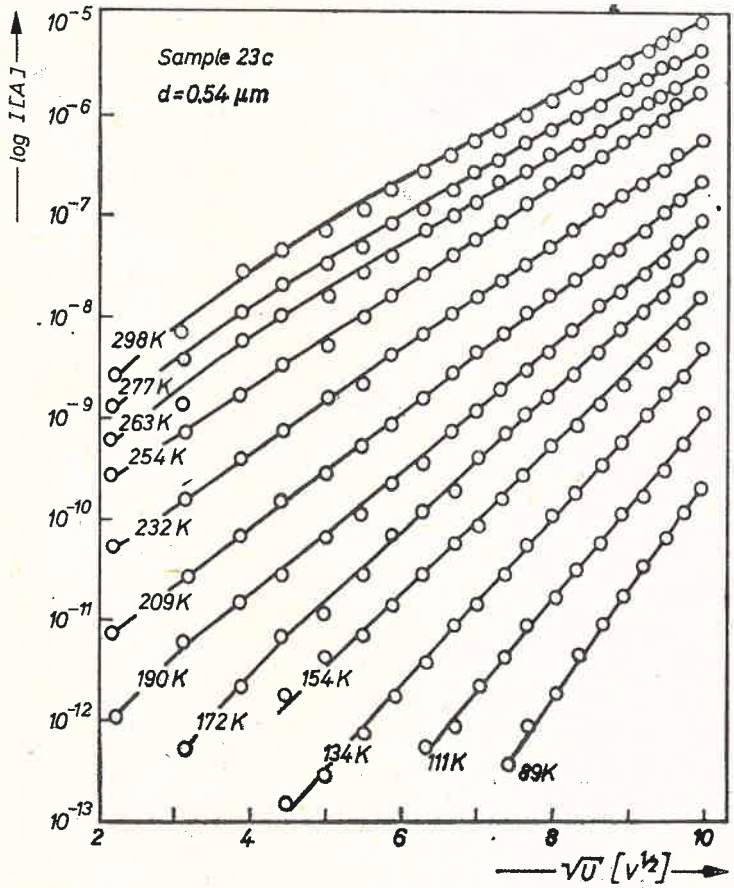

Fig. 5. Dependence of ln I on the square root of voltage for different temperatures

Frenkel from discrete trapping levels [4, 14, 15]. The analytical description of both types of emission is given by the expression [16].

$$J \sim \exp\left(-\frac{\beta V^{1/2}}{kT}\right), \tag{1}$$

and the difference between them is in the coefficient which for the case of the Richardson–Schottky emission is

$$\beta_{R-S} = \left(\frac{e^3}{4\pi\varepsilon}\right)^{1/2}, \tag{2}$$

and for the case of Poole-Frenkel emission

$$\beta_{P-F} = 2\left(\frac{e^3}{4\pi\varepsilon}\right)^{1/2}. \tag{3}$$

The plot of $\log I = f(U^{1/2})$ enables us to calculate the height of the potential barrier at the metal-dielectric boundary [15] (for $U = 0$) as

$$\varphi = -kT \ln\left(\frac{I_0}{S A T^2}\right), \tag{4}$$

where I_0 — cut-off current, T — temperature, S — sample surface, $A = 120\ \mathrm{cm^{-2}K^{-2}}$ — Richardson constant, k — Boltzmann constant

From the expression for current density when the Richardson-Schottky emission assumed

$$j = AT^3 \exp\left(\frac{\beta_{R-S}F^{1/2} - \varphi}{kT}\right), \tag{5}$$

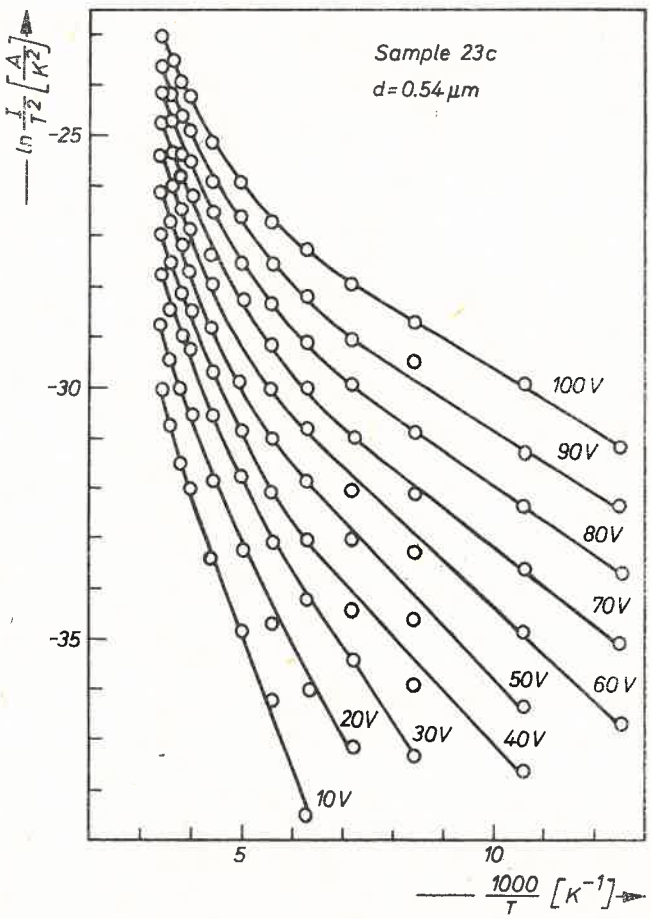

Fig. 6. Dependence of $\ln(I/T^2)$ on the reciprocal temperature

the height of the potential barrier after applying external voltage to the sample can be determined as well [3]. From the plot of the dependence $\ln(I/T^2) = f(1000/T)$ (Fig. 6) we can calculate $(\beta_{R-S}F^{1/2} - \varphi)$. When β_{R-S} is known (Eq. (3)), φ can be determined for a given external voltage.

The calculated heights of the potential barrier at the metal-dielectric interface are in the range 0.8—0.9 eV and do not exhibit any dependence on the kind of metal used for electrodes. This is in agreement with literature data [15].

In the presence of an external electric field, the potential barrier height varies over the range 0.309—0.374 eV when the field varies from 18.6×10^6 V/m to 18.6×10^7 V/m.

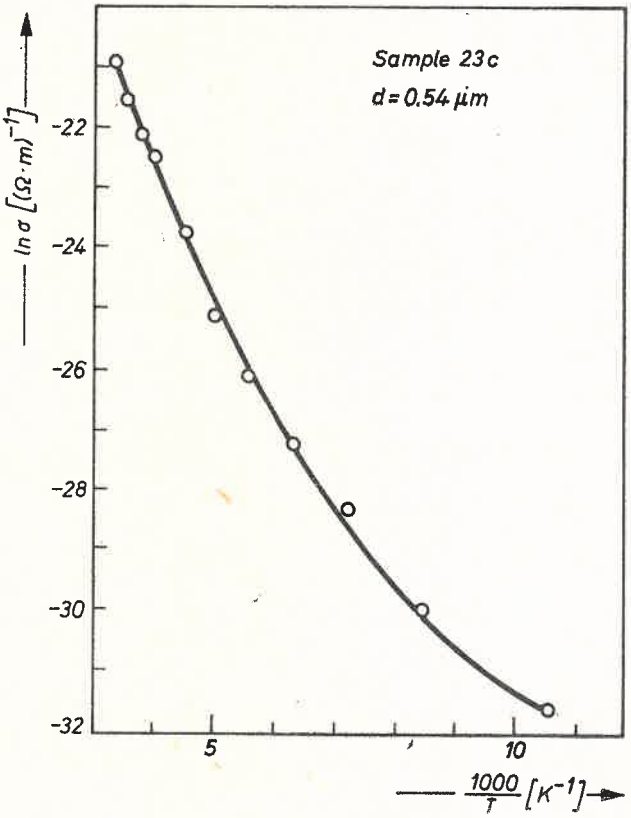

Fig. 7. Temperature dependence of the conductivity

The external electric field evidently has a very strong influence on the height of potential barrier.

From the plot of $\ln \sigma$ versus $1000/T$ (Fig. 7) the activation energies have been calculated. The obtained values are in the range 0.16—0.19 eV and indicate the presence of trapping levels in the energy gap of investigated structures.

3.2. Capacity and ac conductivity

Low-relaxation effects have also been investigated. The measurements were performed in atmosphere using the voltage of 200 mV.

The dependence of capacity on frequency is presented in Fig. 8 for samples of three different thicknesses. From the obtained data the dielectric permeability ε was calculated as 3.47, 5.94 and 9.69 for the samples presented in Fig. 8.

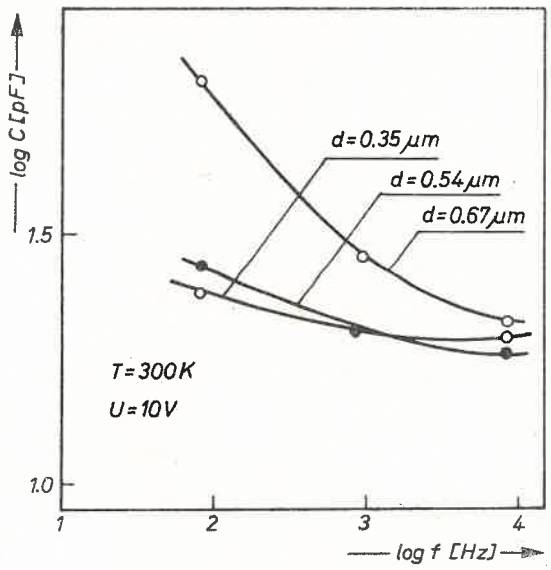

Fig. 8. Dependence of capacity on frequency for films with different thicknesses at room temperature

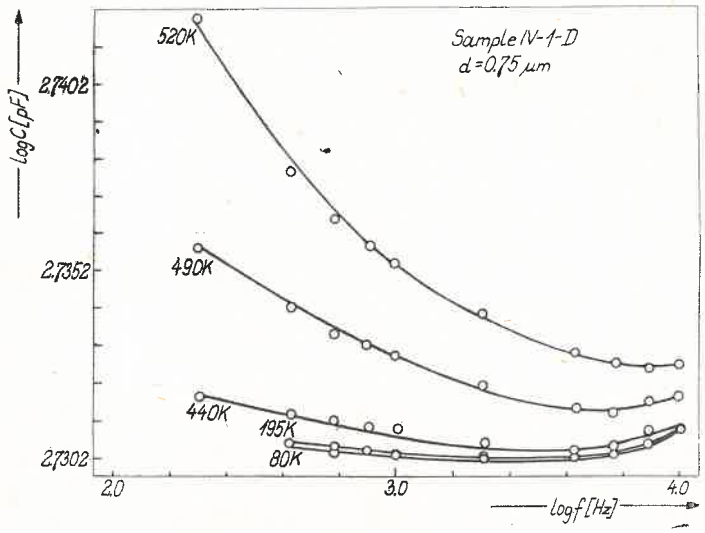

Fig. 9. Dependence of capacity on frequency for different temperatures

The character of $C-f$ dependence is similar to that for the case of vacuum measurements with applied voltage of about 200 mV. This dependence for different temperatures is presented in Fig. 9 and is weakly influenced by temperature over a rather wide range, from liquid nitrogen temperatures up to about 400 K. Above this temperature the dependence becomes stronger. The capacity changes for the entire range of frequencies are contained in one decade.

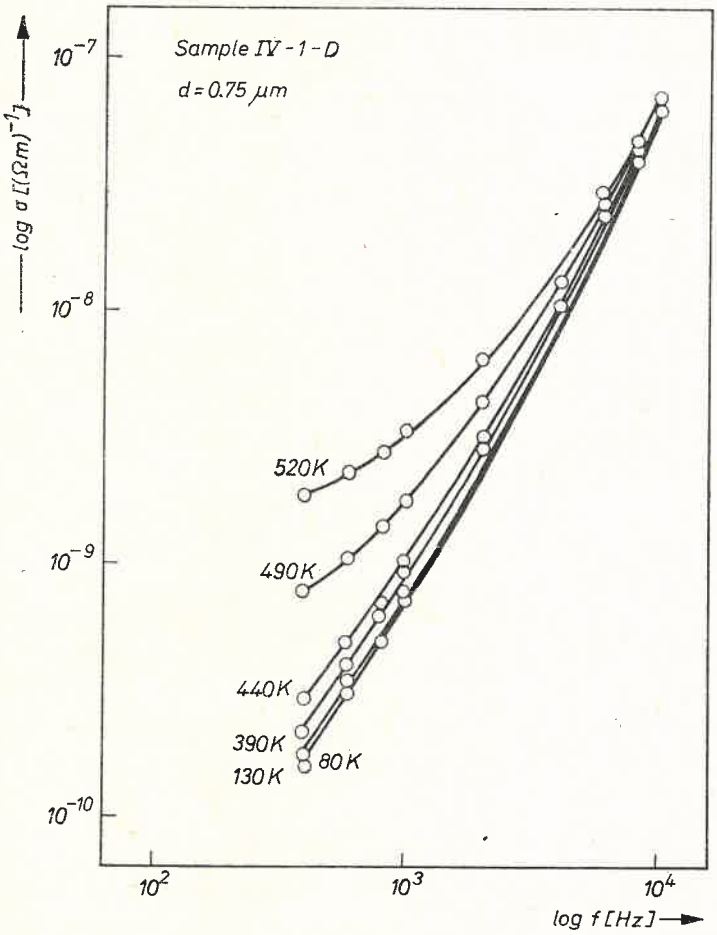

Fig. 10. Dependence of ac conductivity on frequency for different temperatures

In Figs. 10 and 11 the dependences of ac conductivity on frequency and on temperature are presented. The temperature dependence of conductivity is strong for lower frequencies and high temperatures. For higher frequencies this dependence is nearly completely eliminated. Two regions mentioned above are also exhibited on plots of conductivity versus temperature for different frequencies (Fig. 11).

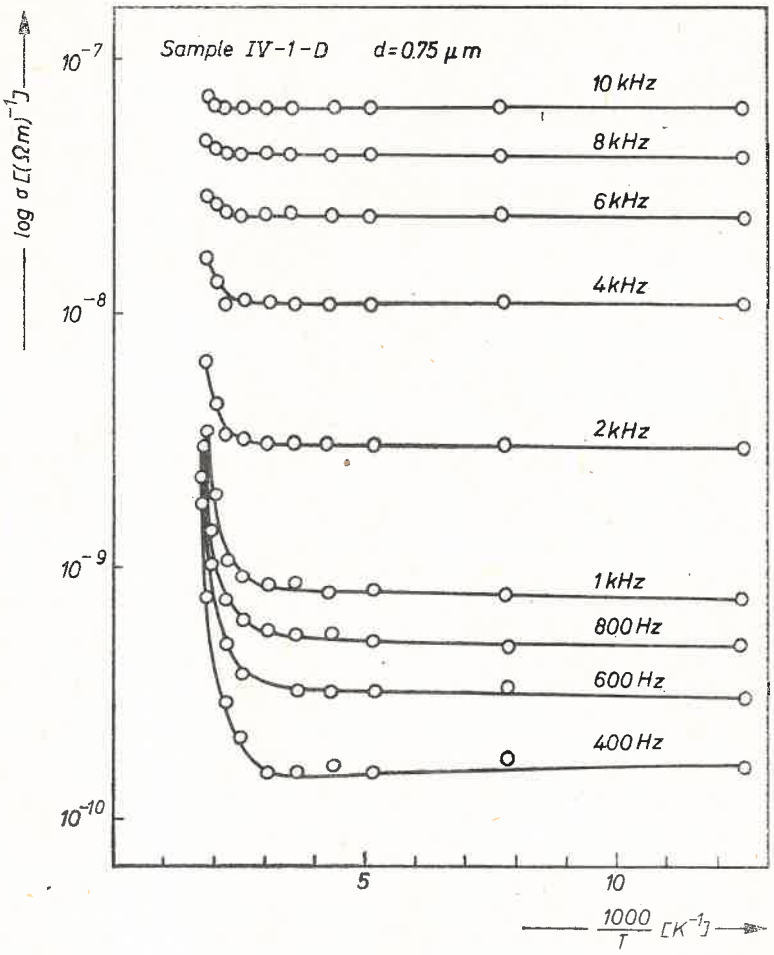

Fig. 11. Dependence of ac conductivity on the reciprocal temperature for different frequencies

4. *Discussion*

The results obtained refer to amorphous films. Reproducibility of determined current-voltage characteristics depends on conditions of measurements. Long-term establishment of current after applying the stationary voltage suggests that the dielectric is in an unstable state. The time of going over from an unstable to a stable state is different for different dielectrics and changes from 10^{-3} s to 10^{12} s [12]. This is due to the trapping of electrons, under the assumption that current carriers are electrons. The time an electron stays in a trap depends on its depth and on temperature. Dielectric relaxation time connected with the relaxation process is given by [17].

$$t_r = 10^{-23} N_t^{1/2} \exp\left[(E_1 - 2\beta F^{1/2})/kT\right], \tag{6}$$

where N_t is the density of traps, E_1 — trapping level depth for zeroth external field, F — external electric field, T — temperature. Expression (6) refers to a dielectric in which only one, accurately determined trapping level is present.

For the case of the investigated SiO_x films the presence of one strictly defined level cannot be assumed, so the time given by Eq. (6) may serve for orientation only. In amorphous materials, to which SiO_x belongs, the traps are deeply lying localized states according to the model presented in [6]. For a stable state at a given temperature, a trapping level characterized by the greatest number of captured electrons is presented. Such a state is established as a result of decreasing density of localized states with increasing distance from the bottom of the conduction band and increase of the occupation time for a given state with increasing depth of this state.

The trapping level, in the above meaning, with the greatest concentration of captured electrons is responsible for low-relaxation processes which are observed when I—V characteristics are taken off. The manner in which the characteristics are determined implies that at low temperatures we deal only with an unstable state and at higher temperatures the measured current corresponds to the stable one.

Linear internal field of dielectrics is characteristic of an unstable state. This enables us to explain the conductivity in terms of the Poole–Frenkel mechanism.

For a stable state it can be assumed that the applied voltage is compensated by the positive spatial charge of empty cathodic space if the voltage is comparable with the difference in work functions for metal and dielectric. In this case the Poole–Frenkel mechanism has little probability.

Since the ranges of applied voltages and temperatures over which the I—V characteristics were determined are rather wide, one should assume that both the Poole–Frenkel and Schottky mechanisms are present. For extreme cases the dominating role may be played by one of them.

This implies that the energy calculated on the basis of Eq. (4) can be ascribed to the height of Schottky or Poole–Frenkel barriers. Ln σ versus $1000/T$ is not a straight line and two extreme values of activation energies (0.12 and 0.19 eV) can be calculated. For the equilibrium state (at low voltage) the height of the Schottky barrier should be determined by these energies.

When the I—V characteristics are analyzed according to Hill's [18] assumptions, then all the observed dependences can be explained in terms of the Poole–Frenkel effect and Poole law. The normalization curve prepared on the basis of $\log I$ versus $\log U$ characteristics for different temperatures is presented in Fig. 12. The general equation which describes such a normalizaton curve is of the form

$$\mathcal{J} = f_n(\alpha, \sinh \alpha),$$

where

$$J = IT^{-n} \exp(E_1/kT) \text{ with } n = 3 \text{ or } 4, \text{ and } E_i = 0.35 \text{ eV}$$

$$\alpha = \beta F^{1/2}/kT.$$

The normalization between field and temperature, $F^{1/2}T^{-1}$, gives definite evidence of the existence of Poole–Frenkel conductivity. Under Poole–Frenkel conductivity the conduction by discrete Coulomb centers is understood [18]. Fig. 12 shows that all the curves from Fig. 4 are parts of one curve and that normalization between field and temperature is of the form $F^{1/2}T^{-1}$ which indicates the presence of single-centered Poole–Frenkel effect.

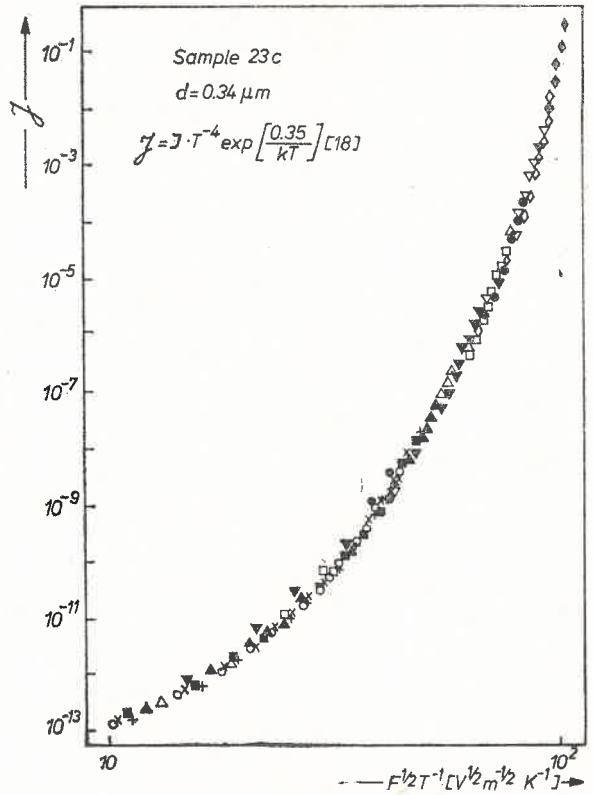

Fig. 12. Normalization curve of current-voltage characteristics (acc. to [18]). Different points denote current-voltage characteristics for different temperatures

The authors are much indebted to Professor W. Żdanowicz for continuous interest in the work and to Professor A. K. Jonscher from Chelsea College of London University for valuable discussion of results. Special thanks are due to B. Wilczak, M. Sc. for help in measurements and to Mrs M. Korona for technical assistance.

REFERENCES

[1] H. Hirose, Y. Wada, *Japan J. Appl. Phys.* **4**, 639 (1965).
[2] I. T. Johansen, *J. Appl. Phys.* **37**, 499 (1966).
[3] J. J. O'Dwyer, *J. Appl. Phys.* **37**, 599 (1966).
[4] T. E. Hartman, J. C. Blair, R. Bauer, *J. Appl. Phys.* **37**, 2468 (1966).
[5] R. A. Morley, D. S. Campbell, *Thin Solid Films* **2**, 403 (1966).

[6] A. K. Jonscher, *Thin Solid Films* **1**, 213 (1967).
[7] F. Argall, A. K. Jonscher, *Thin Solid Films* **2**, 185 (1968).
[8] G. Nåvik, *Thin Solid Films* **6**, 145 (1970).
[9] A. Servini, A. K. Jonscher, *Thin Solid Films* **3**, 341 (1969).
[10] R. M. Hill, *Thin Solid Films* **1**, 39 (1967).
[11] G. Hass, R. E. Thun, *Fizika Tonkikh Plienok*, Izd. Mir, Moskva 1967 (in Russian).
[12] T. Krajewski, *Zagadnienia Fizyki Dielektryków*, WKŁ, Warszawa 1970 (in Polish).
[13] J. G. Simmons, G. W. Taylor, *Phys. Rev.* **B6**, 4793 (1972).
[14] J. G. Simmons, *Phys. Rev.* **155**, 657 (1967).
[15] M. J. Jelinson, *Voprosy Plienochnoy Elektroniki*, Izd. Sov. Radio, Moskva 1966 (in Russian).
[16] A. Adachi, Y. Schibata, S. Ono, *J. Phys.* **D4**, 988 (1971).
[17] J. G. Simmons, C. W. Taylor, *Phys. Rev.* **B6**, 4804 (1972).
[18] R. M. Hill, *Philos. Mag.* **23**, 59 (1971).